

LASER GYROSCOPES

https://doi.org/10.1070/QEL17095

Effect of backscattering on nonlinear distortions of the scale factor of a laser gyro with a rectangular bias

S.E. Beketov, A.S. Bessonov, E.A. Petrukhin, I.N. Khokhlov, N.I. Khokhlov

Abstract. **We report the results of measurements of nonlinear scale factor corrections, resulting from the backscattering effect in a laser gyro with a rectangular bias. It is shown that taking conservative and dissipative backscattering components into account allows one to obtain analytical relationships that adequately describe the frequency response of a laser gyroscope over the entire working range of angular velocities. Using these relationships to correct the frequency response of a laser gyroscope makes it possible to reduce the value of nonlinear corrections to 1–2 ppm.**

Keywords: *ring laser, laser gyroscope, backscattering, scale factor, frequency bias.*

1. Introduction

Backscattering of light by ring cavity (RC) mirrors leads to nonlinear distortions of the frequency response of a laser gyroscope (LG). The most striking manifestation of this physical effect is the so-called frequency locking of counter-propagating waves (CPWs) of a ring laser (RL), which occurs at low rotation velocities [1, 2]. The use of an alternating frequency bias can significantly reduce nonlinear distortion of the frequency response without decreasing the LG sensitivity at low velocities [2, 3].

Currently, two types of alternating biases are widely used. Firstly, this is a harmonic bias, in which an RL is mounted on a mechanical vibrator [2]. Secondly, this is a rectangular bias in the case of an RL with magneto-optical control of the frequency nonreciprocity of the CPWs. An example of this type of a gyroscope is a Zeeman LG [4, 5], where the nonreciprocity is produced by applying a longitudinal magnetic field to the active medium of a laser with a nonplanar RC.

The main distinctive feature of the second type of the bias is significant nonlinear distortions of the LG frequency response at a rotation velocity slightly different from the rectangular bias amplitude. At this rotation velocity, the LG is in the lock-in zone during one of the half-periods of the bias. In calculating the nonlinear correction resulting from backscattering (BS) effects, the value of the scale factor (SF) K at a high rotation velocity Ω of the rotary table (for the LG $\Omega_{\max} \approx 400$ deg s^{-1}) is taken to be unity, and the value of the nonlinear correction is calculated using the relation

$$\Delta K(\Omega) = \frac{K(\Omega)}{K(\Omega_{\max} \to \infty)} - 1\,. \tag{1}$$

Until recently, a theoretical dependence [5, 6]

$$\Delta K(\Omega) = \frac{\Omega_{\mathrm{L}}^2}{2(\Omega_0^2 - \Omega^2)} \tag{2}$$

was used to describe the results of the SF measurements of a Zeeman LG, where Ω_{L} is the threshold lock-in frequency and Ω_0 is the rectangular bias amplitude. Relation (2) describes the left and right wings of the $\Delta K(\Omega)$ dependence for $\Omega < \Omega_0 - \Omega_{\mathrm{L}}$ and $\Omega > \Omega_0 + \Omega_{\mathrm{L}}$, respectively. The central part of the dependence ($\Omega_0 - \Omega_{\mathrm{L}} < \Omega < \Omega_0 + \Omega_{\mathrm{L}}$) is a linear function. At an angular velocity equal to the bias amplitude, the correction is $\Delta K = 0$. According to [5], the maximum and minimum values of the nonlinear correction are expressed as

$$\Delta K_{\max,\min} = \pm 20\left(\frac{\Omega_{\mathrm{L}}}{\Omega_0}\right)^2. \tag{3}$$

Figure 1 shows the $\Delta K(\Omega)$ dependence for typical values of the parameter ($\Omega_{\mathrm{L}} = 0.1$ deg s^{-1} and $\Omega_0 = 30$ deg s^{-1}) of the MT-501 gyroscopic sensor developed at the Polyus Research Institute.

From our point of view, the correctness of relation (3) is doubtful. In particular, Khoshev [6] presents the following estimate for the maximum and minimum values of the nonlinear correction:

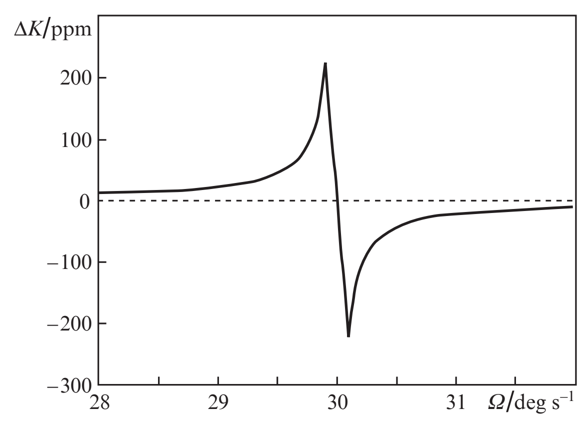

Figure 1. Calculated dependence of the nonlinear SF correction for the LG with a rectangular bias on the angular velocity.

S.E. Beketov, A.S. Bessonov, E.A. Petrukhin, I.N. Khokhlov, N.I. Khokhlov OJSC M.F. Stel'makh Polyus Research Institute, ul. Vvedenskogo 3, 117342 Moscow, Russia; e-mail: petruhin53@mail.ru

Received 14 July 2019; revision received 11 August 2019
Kvantovaya Elektronika **49** (11) 1059–1067 (2019)
Translated by I.A. Ulitkin

$$\Delta K_{\max,\min} \approx \pm 0.15 \frac{\Omega_{\rm L}^2}{\Omega_0 F}, \tag{4}$$

where F is the switching frequency of the rectangular bias (the frequency in Hz must be converted into deg s^{-1}).

The value of this correction can also be estimated within the framework of the model of the quasi-stationary sign switching regime of the rectangular bias. At a low switching frequency (for definiteness, less than 1 Hz), the influence of parametric resonances can be neglected and use can be made of the classical dependence of the RL beat frequency on the rotation velocity:

$$\Delta\nu = \sqrt{(\Omega \pm \Omega_0)^2 - \Omega_{\rm L}^2}. \tag{5}$$

The signs $\pm$ refer to half-periods of a slowly switching rectangular bias. We assume that half the time t the sign of the LG bias is positive, and half the time it is negative. Then for the nonlinear correction to the SF we have the relation:

$$\Delta K = \frac{0.5t\sqrt{(\Omega - \Omega_0)^2 - \Omega_{\rm L}^2} + 0.5t\sqrt{(\Omega + \Omega_0)^2 - \Omega_{\rm L}^2}}{\Omega t} - 1. \tag{6}$$

This relation is written for the case when the LG is outside the lock-in zone, that is, when $|\Omega - \Omega_0| \geqslant \Omega_{\rm L}$ (without loss of generality, we assume that $\Omega > 0$). Inside the lock-in zone, the first term in the numerator of fraction in (6) becomes equal to zero. It is easy to verify that the maximum and minimum values of the nonlinear SF correction are reached at rotation velocities $\Omega = \Omega_0 \pm \Omega_{\rm L}$ and are equal to

$$\Delta K_{\max,\min} = \pm 0.5 \frac{\Omega_{\rm L}}{\Omega_0}. \tag{7}$$

As can be seen from a comparison of relations (3), (4) and (6), they yield mutually exclusive estimates of both the magnitude and functional dependences. We should also add here the results of calculations and experiments presented in [7]. The authors of this work showed that the central part of the $\Delta K(\Omega)$ dependence comprises several parametric lock-in zones of comparable width. They note that the central part of the dependence is not a monotonic function and the width of the oscillation region caused by the influence of parametric resonance zones is noticeably larger than that of the lock-in zone.

It is also worth noting that the nonlinear distortions of the SF of this LG type exceed several hundred ppm. Such a significant scale of nonlinear distortions makes the use of the SF correction in an LG with a rectangular bias quite important. However, to do this, LG developers must rely on a physical model that adequately describes the influence of BS effects. The development of such a model is the main task of this work.

2. Results of measurement and modelling of nonlinear SF corrections of a Zeeman LG

The SF of uniaxial MT-501 sensors was measured using standard measuring equipment developed at the Polyus Research Institute. In these measurements, by the SF is meant the number of pulses of the SPW beat signal when the sensor is rotated through an angle that is a multiple of 360° (up to several full revolutions). To eliminate the effect of the LG zero shift, two SF measurements were performed – with the sensor rotating clockwise and counterclockwise. The SF value was the half-sum of the obtained values. In determining the value of the nonlinear correction, the SF value at an angular velocity of 400 deg s^{-1} was taken as unity and the correction was calculated by formula (1). The sensors were mounted on a rotary table, the relative deviation of the rotation velocity of which did not exceed 0.001 %. The error in the measurements of the nonlinear SF correction was less than or equal to 2–3 ppm.

Figure 2 shows one of the measured $\Delta K(\Omega)$ dependences. Three characteristic areas of this dependence can be distinguished: the central part near the bias amplitude with a width of about 1–2 deg s^{-1}, as well as the right and left wings, corresponding to rotation velocities higher and lower than the bias amplitude. With all the variety of the shape of these dependences for different sensors, they are easy to classify. We investigated several dozen MT-501 sensors. The central part of the dependence has the most complex shape. We will describe it later. Let us now consider in more detail the wings of the $\Delta K(\Omega)$ dependence. In Fig. 3, the solid curves correspond to the wings of this dependence for one of the sensors. Dashed curves indicate the boundaries inside which there are the wings of the dependences for all studied sensors. It is easy to see that the theoretical dependence shown in Fig. 1 differs significantly from that observed experimentally. First of all, this concerns the positive SF correction characteristic of most sensors on the right wing of the dependence, while relation (2) gives a negative sign of the correction. To understand the reason for this difference, we turn to the system of equations describing intensities and phase differences of the RL counterpropagating waves [2, 3, 6]:

$$\frac{{\rm d}t_{\rm cw}}{{\rm d}t} = I_{\rm cw}\frac{c}{L}\left[(\alpha - \delta) - \beta I_{\rm cw} - \theta I_{\rm ccw} + 2r_{\rm ccw}\left(\frac{I_{\rm ccw}}{I_{\rm cw}}\right)^{1/2}\cos(\psi + \varphi_{\rm ccw})\right], \tag{8}$$

$$\frac{{\rm d}t_{\rm ccw}}{{\rm d}t} = I_{\rm ccw}\frac{c}{L}\left[(\alpha - \delta) - \beta I_{\rm ccw} - \theta I_{\rm cw} + 2r_{\rm cw}\left(\frac{I_{\rm cw}}{I_{\rm ccw}}\right)^{1/2}\cos(\psi - \varphi_{\rm cw})\right], \tag{9}$$

$$\frac{{\rm d}\psi}{{\rm d}t} = \Omega + \frac{c}{L}\left[r_{\rm ccw}\left(\frac{I_{\rm ccw}}{I_{\rm cw}}\right)^{1/2}\sin(\psi + \varphi_{\rm ccw}) + \right.$$

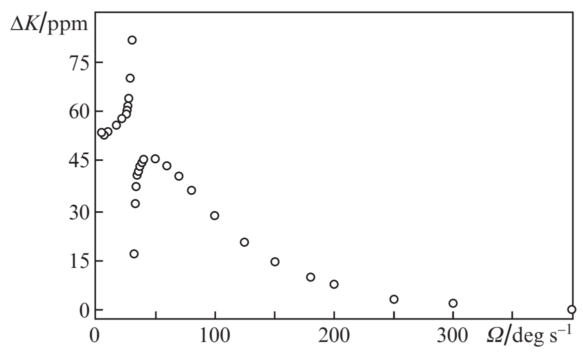

Figure 2. Dependence of the nonlinear correction ΔK on the angular velocity of the MT-501 sensor.

$$+ r_{\rm cw}\left(\frac{I_{\rm cw}}{I_{\rm ccw}}\right)^{1/2}\sin(\psi - \varphi_{\rm cw})\Bigg], \tag{10}$$

where $I_{\rm cw}$ and $I_{\rm ccw}$ are the intensities of the RL counterpropagating waves passing in the clockwise and counterclockwise direction; ψ is the phase difference of the CPWs; α is the gain of the active medium; and δ is the RC loss. Coefficients β and θ are parameters of nonlinear self-saturation and mutual saturation of CPWs in the active medium, respectively; c is the speed of light; and L is the RC perimeter.

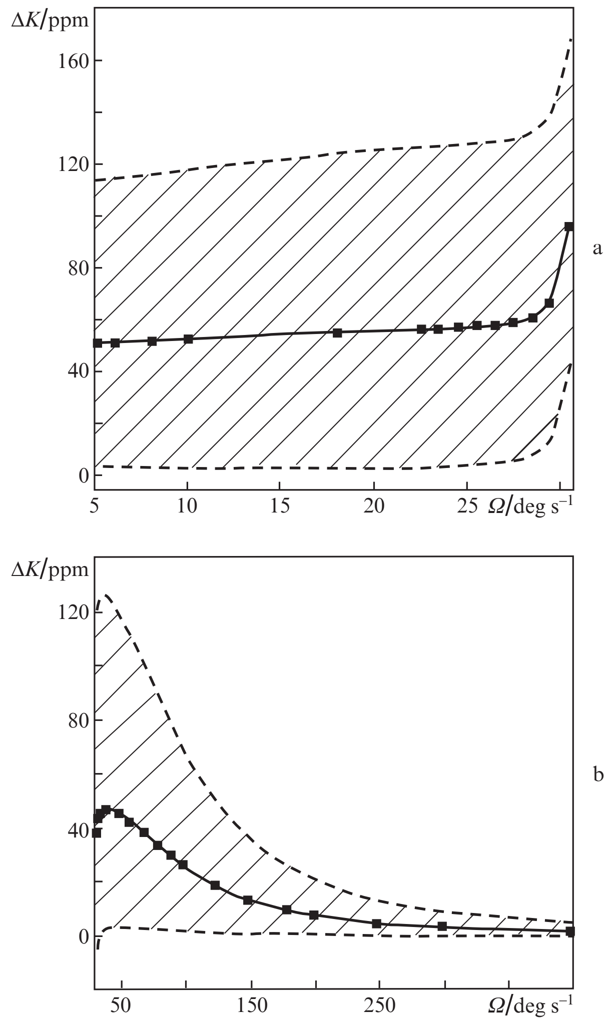

Figure 3. (a) Left and (b) right wings of the $\Delta K(\Omega)$ dependence for the MT-501 sensor (solid lines) and the boundaries of the dependences for the array of sensors in question (dashed lines). Points are the measurement results.

The BS effect is described by two complex coupling parameters (CCPs), which are parts of the natural oscillation field scattered in the opposite direction:

$$\tilde{r}_{\rm cw} = r_{\rm cw}\exp(\mathrm{i}\varphi_{\rm cw}), \tag{11}$$

$$\tilde{r}_{\rm ccw} = r_{\rm ccw}\exp(\mathrm{i}\varphi_{\rm ccw}). \tag{12}$$

In the weak coupling approximation, when the beat frequency of CPWs significantly exceeds the lock-in threshold, the system of equations (8)–(10) can be solved by the small perturbation method. As a result, we obtain the relation for the LG beat frequency:

$$\Delta\nu = \Omega - \left(\frac{c}{L}\right)^2\left(\frac{S_+^2}{2\Omega} - \frac{1}{2}\frac{S_-^2\Omega}{\Omega_{\rm g}^2 + \Omega^2}\right), \tag{13}$$

where Ω is the frequency bias in rad s^{-1}. The parameter $\Omega_{\rm g}$ is called the strength of the limit cycle and is determined by the expression

$$\Omega_{\rm g} = \Delta\Omega_{\rm c}\frac{\alpha - \delta}{\delta}\frac{\beta - \theta}{\beta + \theta}, \tag{14}$$

where $\Delta\Omega_{\rm c} = c\delta/L$ is the RC bandwidth. Parameters S_+ and S_- are CCP combinations:

$$S_+ = \sqrt{r_{\rm cw}^2 + r_{\rm ccw}^2 + 2r_{\rm cw}r_{\rm ccw}\cos(\varphi_{\rm cw} + \varphi_{\rm ccw})}, \tag{15}$$

$$S_- = \sqrt{r_{\rm cw}^2 + r_{\rm ccw}^2 - 2r_{\rm cw}r_{\rm ccw}\cos(\varphi_{\rm cw} + \varphi_{\rm ccw})}. \tag{16}$$

In the theory of ring gas lasers (see, for example, [8]), two types of BS sources are considered, i.e. dissipative and conservative. Their difference lies in the magnitude of the CPW phase shift during backscattering. For dissipative and conservative sources, the phase shifts are π ($\varphi_{\rm cw} = \varphi_{\rm ccw} = \pi$) and $\pi/2$ ($\varphi_{\rm cw} = \varphi_{\rm ccw} = \pi/2$), respectively. In a real RC, the fields of BS waves are formed as a result of interference of waves scattered from sources of both types. In this case, the total modulus of the CCP of dissipative BS sources is $r = S_+/2$, and of conservative ones – $R = S_-/2$. It is easy to see that the lock-in threshold for the RL is determined by the presence of dissipative BS sources on the RC mirrors. In the language of the system of equations (8)–(10), the lock-in threshold $\Omega_{\rm L}$ is determined by the relation

$$\Omega_{\rm L} = \frac{c}{L}S_+. \tag{17}$$

If we now turn to relation (13), we can see that dissipative and conservative BS sources yield SF corrections of different signs for the LG. The correction for dissipative sources has a negative sign, and for conservative sources it is positive. When modelling the parametric LG effects with an alternating bias, the influence of conservative BS sources is neglected. As a result of simplifications, equation (10) is reduced to the well-known phase equation:

$$\frac{\mathrm{d}\psi}{\mathrm{d}t} = \Omega + \Omega_{\rm L}\sin\psi. \tag{18}$$

This equation does not make it possible to explain the positive sign of the correction for the right wing of the $\Delta K(\Omega)$ dependence.

Using relation (13), we can determine the $\Delta K(\Omega)$ dependence for the 'quasi-stationary' (slow) sign switching regime of a rectangular bias. To this end, we must take into account the fact that during the time t of the LG rotation by the angle $\Phi = \Omega t$, the value of the bias is equal to $\Omega - \Omega_0$ during one half of the time and to $\Omega + \Omega_0$ during the other. Accordingly, for the CPW beat frequency, we have

$$\Delta\nu(\Omega - \Omega_0) = (\Omega - \Omega_0) - \frac{S_+^2}{2(\Omega - \Omega_0)} + \frac{S_-^2(\Omega - \Omega_0)}{2[(\Omega - \Omega_0)^2 + \Omega_{\rm g}^2]}, \tag{19}$$

$$\Delta\nu(\Omega+\Omega_0) = (\Omega+\Omega_0) - \frac{S_+^2}{2(\Omega+\Omega_0)} + \frac{S_-^2(\Omega+\Omega_0)}{2[(\Omega+\Omega_0)^2+\Omega_g^2]}. \tag{20}$$

By summing the number of pulses of the beat signal over time t, the above formula (6) is obtained.

After further calculations, we arrive at the relation describing the left and right wings of the $\Delta K(\Omega)$ dependence:

$$\Delta K = \frac{S_+^2}{2(\Omega_0^2-\Omega^2)} + \frac{S_-^2(\Omega_g^2+\Omega^2-\Omega_0^2)}{2[(\Omega-\Omega_0)^2+\Omega_g^2][(\Omega+\Omega_0)^2+\Omega_g^2]}. \tag{21}$$

Using this relation makes it possible to quantitatively and qualitatively approximate in an analytical form the measured $\Delta K(\Omega)$ dependences. Thus, we developed a computational program that allows us to solve the inverse problem: to determine the parameters S_-, S_+ and Ω_g directly from the measured $\Delta K(\Omega)$ dependence. In this case, the standard deviation of the difference between the measured and approximated values, as a rule, did not exceed 1–2 ppm. As for the value of Ω_g, in our experiments we used sensors with approximately the same pressure and composition of the gas mixture, RC losses and discharge current. In approximating the $\Delta K(\Omega)$ dependences, we used $\Omega_g = 75$ deg s^{-1}.

Figure 4 shows several examples of approximation of the results of measurements of the wings of the $\Delta K(\Omega)$ dependence. The shape of the right wing is determined mainly by the ratio of the parameters S_- and S_+. At $S_-/S_+ > 5$, a characteristic maximum is observed at a rotation velocity of 40–50 deg s^{-1}. If the conservative BS component slightly (two to three times) exceeds the dissipative component, the SF correction for the right wing has a negative sign in the entire velocity interval.

The S_- and S_+ parameters for the sensors in question varied in the ranges 0.1–1.4 deg s^{-1} and 0.03–0.20 deg s^{-1}, respectively. For some sensors, we observed a slight difference in the S_- and S_+ values obtained by approximating the right and left wings. This difference did not exceed 10%–15%.

It should be noted that, depending on the conditions of the problem, the dimension of the parameters S_- and S_+ can vary. In the case of relations (15) and (16), the CCP moduli are the ratio of the amplitudes of the backward and forward waves and are expressed in units of ppm. In measuring nonlinear SF corrections, nonlinear corrections are present in the

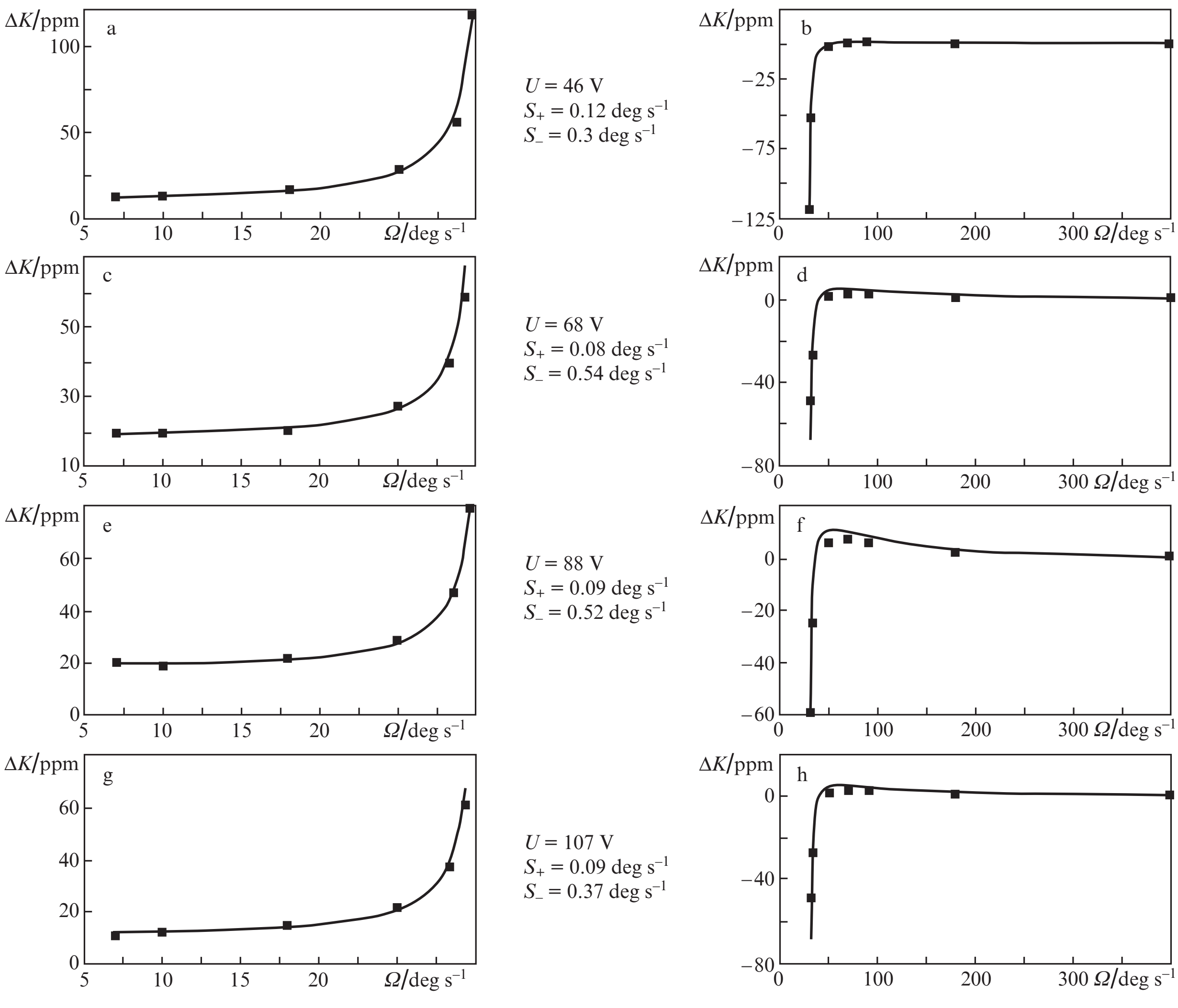

Figure 4. (a, c, e, g) Left and (b, d, e, h) right wings of the $\Delta K(\Omega)$ dependence for four adjacent modes of the MT-501 sensor. Points are the measurement results, solid lines are the results of calculations by formula (21) at $\Omega_g = 75$ deg s^{-1}. The indicated voltages U at the piezoelectric correctors correspond to the central position of the RL mode.

initial equations in the form of their ratio to the angular velocity. Therefore, for greater visibility of the CCPs, it is better to use degrees per second.

Of course, such a good coincidence of the approximated and measured dependences does not allow us to state that we found an exact analytical relation to describe nonlinear SF corrections of the LG with an alternating bias. First of all, it is necessary to check how much the found parameters S_-, S_+ and Ω_g are related to the parameters (r_{cw}, r_{ccw}, φ_{cw}, φ_{ccw}, α, δ, β and θ) that appear in the system of equations (8)–(10). The issue of using this system of equations, which is derived under the assumption that the excess of gain over losses in the RL is small, also raises doubts. In particular, in [2], the excess $\eta = (\alpha/\delta - 1) < 0.2$ was considered to be a criterion of smallness. Under real conditions of LG operation, this value is an order of magnitude larger.

First, it is necessary to compare the strength of the limit cycle Ω_g obtained by approximation with its calculated value (14). To this end, it is necessary to determine the values of three parameters: RC loss, δ; gain of the active medium, α; and the ratio of the parameters of mutual saturation and self-saturation, θ/β.

The cavity losses of the sensors under study were ~2000 ppm and were determined on the basis of measurements of the resonance width of the radiation intensity emerging from the RC. For a four-mirror RC with a perimeter L = 20 cm and losses of ~2000 ppm, the RC bandwidth is $\sim 3 \times 10^6$ rad s^{-1}, which, in terms of the angular velocity, is ~360 deg s^{-1}. In determining the value of α, we assumed that the CPW intensities in the RL slightly differ ($I_{cw} \approx I_{ccw} = I_0$) and, as follows from the solution of the system of equations (8)–(10), are related to the parameters α and β as follows:

$$I_0 = \delta \frac{\alpha/\delta - 1}{\beta + \theta} = \delta \frac{\eta}{\beta + \theta}. \quad (22)$$

In dc discharge LGs, there are two identical discharge gaps. Therefore, turning off one of them (at a constant discharge current in the discharge gap), there occurs a twofold decrease in the coefficient of unsaturated gain. Measurement of the intensity ratio in these two cases makes it possible to determine the value of η by using relation (22). To meet the conditions for our experiments with LGs with a rectangular bias, we used the parameter $\eta \approx 1.5$ or gain $\alpha \approx 5000$ ppm in normal LG operation.

The ratio of the parameters of mutual saturation and self-saturation θ/β was determined from measurements of the modulation components of the RL intensity with the beat frequency. In the beating regime, the intensities of the waves emerging from the RL can be represented as

$$I_{cw,ccw} = I_0[1 + m_{cw,ccw}\sin(\Delta\nu t + \chi_{cw,ccw})], \quad (23)$$

where I_0 is the constant component of the intensity (we neglect the difference in the constant components of the CPW intensity); $m_{cw,ccw}$ are the modulation depths; and $\chi_{cw,ccw}$ are the phase shifts of modulation components.

If the strength of the limit cycle Ω_g significantly exceeds the value of the bias, then the modulation depth can be expressed as [4, 6]:

$$m_{cw,ccw} = \frac{\sqrt{\beta^2 r_{cw}^2 + \theta^2 r_{ccw}^2 - 2\beta\theta r_{cw} r_{ccw}\cos(\varphi_{cw} + \varphi_{ccw})}}{\Omega_g(\beta + \theta)}. \quad (24)$$

In determining the θ/β ratio, we used the method described in [9]. Using a retroreflecting mirror installed near the output mirror of the RL produced a unidirectional coupling regime. In this case, the CCP modulus of one of the waves (for definiteness, the clockwise wave) significantly exceeds the CCP modulus of the counterclockwise wave. It is easy to verify that the ratio of the modulation depths of SPWs has the form

$$m_{ccw}/m_{cw} = \theta/\beta. \quad (25)$$

In our case, the ratio θ/β was ~0.5. In this case, we used a ^{3}He–^{20}Ne mixture at a pressure of 4.5 Torr and a ratio of partial pressures of helium and neon of 14 : 1. Note that in the above-mentioned work [9], approximately the same value of θ/β was obtained at the same pressure in a mixture with an equal content of ^{20}Ne and ^{22}Ne isotopes.

Using the obtained values of the parameters α, β and θ/β, we can compare the calculated and measured values of the strength of the limit cycle of the sensors. The result of this comparison is presented in Fig. 5. The significant difference between the calculated dependence $\Omega_g(\eta)$ and the results of approximation of the experimentally measured dependences $\Delta K(\Omega)$ at a large excesses of gain over losses is striking. For $\eta \lesssim 0.3$, they practically coincide. At large η, an increase in Ω_g slows down. The dashed line represents the nonlinear dependence, with which we tried to approximate the experimental results:

$$\Omega_g = A\frac{\eta}{1 + 0.9\eta}, \quad (26)$$

where A = 120 deg s^{-1}. With infinitely large growth, the value of Ω_g tends to a value equal to A/0.9.

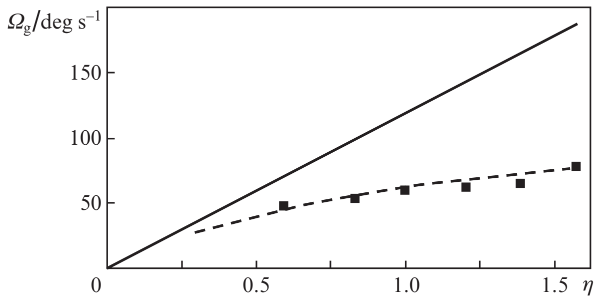

Figure 5. Dependences of the strength of the limit cycle on the excess of gain over losses for the Zeeman LG MT-501. The solid line is the calculation result using relation (14), the dashed line is the calculation result taking into account saturation, and the squares are the result of approximating the experimental dependences $\Delta K(\Omega)$.

Such a significant difference between the measured and calculated values of the strength of the limit cycle raises the question of the legality of using the system of equations (8)–(10) to determine the parameters S_+ and S_-. Is there a relation between their values obtained by approximating the $\Delta K(\Omega)$ dependence and the excess of gain over losses η? Recall that the parameters S_+ and S_- characterise backscattering in the RL and should not depend on the excess of η. Our experiments did not find such a relationship. When the parameter η changes from 0.3 to 2.0, the relative change in the BS parameters did not exceed 10% and could be attributed to the approximation errors of the $\Delta K(\Omega)$ dependences.

Parameters S_+ and S_- can also be determined using relation (21) for the $\Delta K(\Omega)$ dependence in an LG without a bias. This method is well suited in the case of a significant difference in the parameters S_+ and S_-. It is desirable that the S_- value is more than three to five times higher than the dissipative BS component S_+. In this case, the $\Delta K(\Omega)$ dependence contains a pronounced maximum (Fig. 6), the position of which is determined by the strength of the limit cycle Ω_g. The contrast of this dependence also increases with decreasing discharge current, which is accompanied by a decrease in Ω_g.

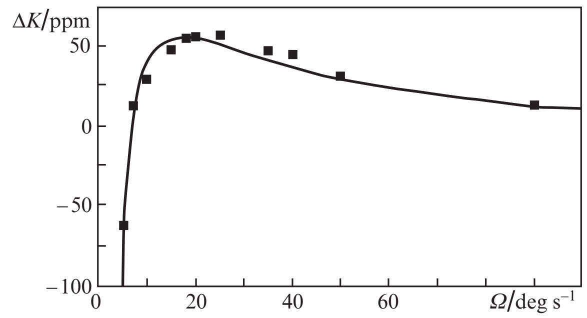

Figure 6. Dependence $\Delta K(\Omega)$ for an LG without a bias at $S_+ = 0.08$ deg s^{-1}, $S_- = 0.48$ deg s^{-1} and $\Omega_g = 38$ deg s^{-1}. Squares are the measurement results, and the solid line is the approximation.

If the condition $S_-/S_+ > 5$ is fulfilled (note that more than half the studied sensors met this condition), no significant difference was found between the BS parameters for LGs with an alternating bias and without a bias.

Another method for estimating the S_- parameter was implemented in the analysis of the variable components of the RL intensity with the beat frequency. It follows from relation (24) at $S_- \gg S_+$ that $m_{cw} \approx m_{ccw} = m$ and the modulation depth is described by the relation

$$m = \frac{S_-}{2\Omega_g}. \tag{27}$$

Based on the results of the modulation depth measurements, we can find the parameter S_-. When comparing the thus found values of S_- and the values of S_- obtained by approximating the $\Delta K(\Omega)$ dependences, we did not observe a large differences between them (it did not exceed 10%–15%).

Let us summarise an intermediate result of our study. A nonlinear dependence of the strength of the RL limit cycle on the excess of gain over loss η was found. This casts doubt on the appropriateness of applying the system of equations (8)–(10) to describe the amplitude–phase characteristics of RLs operating at large values of η. Using the value of the strength of the limit cycle, obtained taking into account the saturation effect, allows one to correctly determine the value of nonlinear SF corrections associated with the influence of backscattering. To describe the wings of the $\Delta K(\Omega)$ dependence, it suffices to use the relation obtained for the regime of 'quasi-stationary' (slow) sign switching of a rectangular bias. The shape of the wings of the $\Delta K(\Omega)$ dependence is determined by four parameters: the dissipative (S_+) and conservative (S_-) BS components, the strength of the limit cycle Ω_g and the rectangular bias amplitude Ω_0.

Let us now consider the central part of the $\Delta K(\Omega)$ dependence (Fig. 7a). Its nonmonotonic behaviour makes it difficult to introduce nonlinear SF corrections. Such a complex form of parametric lock-in zones is almost impossible to describe using a convenient and, from a physical point of view, correct analytical relationship. The only way out of this situation, in our opinion, is related to the introduction of 'dithering noise' of the frequency bias amplitude. The width of the region where parametric resonances appear is 1–1.5 deg s^{-1}. Therefore, the optimal value of the amplitude of dithering noise should approximately correspond to this value. In our case, we used quasi-noise by introducing an amplitude-modulated harmonic signal into the correcting solenoid of a Zeeman LG:

$$\Omega_n = \Omega_a \sin(2\pi f_1)\sin(2\pi f_2), \tag{28}$$

where $f_1 = 200$ Hz; $f_2 = 45$ Hz; and $\Omega_a \approx 1.2$ deg s^{-1}.

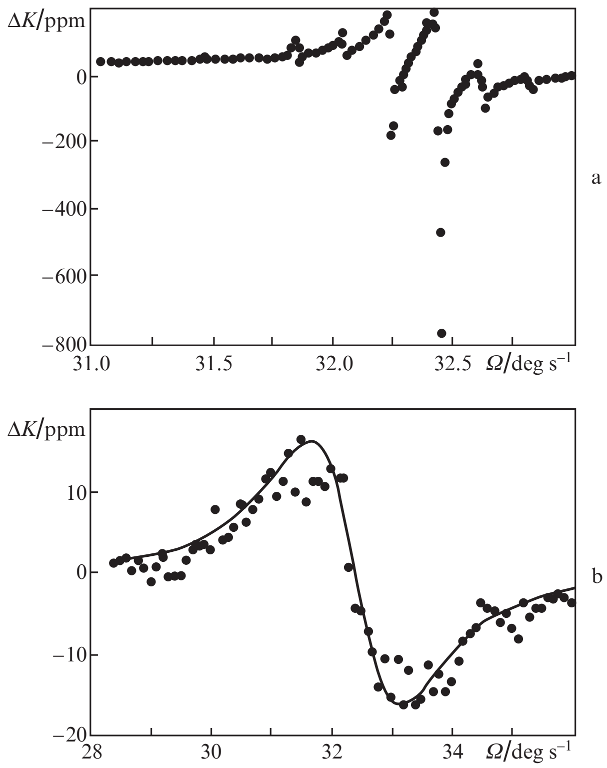

Figure 7. Central part of the $\Delta K(\Omega)$ dependence (a) without noise and (b) after the introduction of dithering noise. Points are the measurement results, and the solid line is the approximation.

With such a dithering noise, the parametric lock-in zones disappear (Fig. 7b), and the peak value of the nonlinear correction $\Delta K(\Omega)$ decreases by almost two orders of magnitude, reaching 30 ppm. The shape of the central part of the $\Delta K(\Omega)$ dependence obtained by introducing the dithering noise is well described by the analytical relation, which is the first derivative of the Lorentz function:

$$\Delta K = -\frac{Nx}{1+x^4}, \tag{29}$$

where

$$x = \frac{\Omega - \Omega_0}{\Omega_a} \tag{30}$$

is the dimensionless detuning of the rotation frequency from the amplitude of the LG bias, and the parameter N linearly depends on the LG lock-in threshold. The shape of this dependence is determined by the dithering noise amplitude Ω_a (Ω_a = 1.2 deg s^{-1}). The presence of the conservative component S_- leads to the appearance of a small bias between the asymptotic values at low and high rotation velocities: $\Delta K(\Omega \to 0) - \Delta K(\Omega \to \infty)$. In the above example, this value was ~10 ppm.

The standard deviation of the difference between the measured and calculated values of the middle part of the $\Delta K(\Omega)$ dependence did not exceed 2 ppm. Thus, the use of analytical relations (21) and (29) allows one to correct significantly (from hundreds to units of ppm) the value of nonlinear SF corrections in the entire working range of rotation velocities of LGs with a rectangular bias.

The next section is devoted to the study of the mechanism of the formation of dissipative and conservative CCP components in the RC. This will help find ways of practical implementation of the SF correction procedure for a Zeeman LG with a rectangular bias.

3. Peculiarities of the formation of conservative and dissipative CCP components in a Zeeman LG

The values of the dissipative and conservative CCP components are determined by the combination of all BS sources located on the surface of the mirrors and falling into the working zone of the CPW modes. We will use the simplest model of the formation of BS fields and will assume that on the surface of each of the RC mirrors there are two point BS sources: dissipative and conservative. The complex coupling coefficients in the system of equations (8)–(10) are the scalar sum of the partial CCPs of individual RC mirrors:

$$r = \sum_n r_n \exp(2\mathrm{i}kl_n), \tag{31}$$

where $k = 2\pi/\lambda$ is the wave number; l_n is the longitudinal coordinate of a point BS source on the optical axis of the RC. In this case, by partial CCP moduli of the mirrors, r_n, are meant their dissipative or conservative component. Relation (31) for them remains the same in form with only the parameters r_n and l_n changing. A factor of 2 in the exponent means that the phase shift for a wave propagating in the opposite direction is doubled compared to the case of interference of waves propagating in the forward direction.

If we represent relation (31) in the form of partial CCP vectors located on a complex plane, then the arguments $2kl_n$ are the angles of rotation of the partial CCPs with respect to each other. In changing the lengths of the cavity arms (for example, under thermal effects), these angles can vary in the range $0-2\pi$. As a result, the moduli of the total CCP can (hypothetically) vary in the range $0-\sum_n r_n$.

We now specify our problem and consider the interference of BS waves in a four-mirror RC of square shape. It is easy to see that in the case of uniform thermal deformations, we observe a periodic change in the modulus of the total CCP. In terms of a change in the RC perimeter, this period is 2λ. Moreover, each vector of partial CCPs rotates on the complex plane by 360°.

To control the perimeter and stabilise it, part of the cavity mirrors is equipped with piezoelectric correctors (PECs). In modern LGs, use is made, as a rule, of a RC with two PECs. In this case, there are two layout options for PECs located either diagonally in the square or on adjacent cavity mirrors. These layout options react differently to uniform thermal deformations (for example, to heating) of the RC (Fig. 8). In the case of a diagonal arrangement of PECs, the optical perimeter turns from a square into a rhombus with the same shoulder length, while the total CCP remains unchanged. In the case of the second layout, the square optical perimeter turns during the heating into a rectangular one. The total CCP changes as follows:

$$r = r_1 + r_2 \exp\left[2\mathrm{i}k\left(l_{12} - \frac{\Delta L}{4}\right)\right] + r_3 \exp\left[2\mathrm{i}k\left(l_{12} + l_{23} - \frac{\Delta L}{4}\right)\right]$$
$$+ r_4 \exp[2\mathrm{i}k(l_{12} + l_{23} + l_{34})]. \tag{32}$$

Here, l_{12}, l_{23} and l_{34} are the distances between the scatterers before heating the cavity (as we called uniform thermal deformation), and ΔL is the change in the RC perimeter with the stabilisation system switched off.

If we group in relation (32) the first term with the fourth one, and the second term with the third one and plot them in the form of two vectors on the complex plane (Fig. 8b), then when the cavity is heated, the total vector $\boldsymbol{r}_{23} = \boldsymbol{r}_2 + \boldsymbol{r}_3$ describes a circle around the total vector $\boldsymbol{r}_{14} = \boldsymbol{r}_1 + \boldsymbol{r}_4$. Therefore, the problem is reduced to the interference of two BS sources with a variable phase varying in the range from 0 to 2π. The modulus of the total CCP will vary in the range from the sum of the moduli of these two vectors to their difference.

An important distinctive feature of the layouts with two PECs is the change in the total CCP during the transition to a neighbouring longitudinal mode (q so-called jump by λ). In this case, there are two possible configurations of partial CCPs (Figs 8c and 8d). The relations for the total CCPs have the form

$$r = r_1 + r_2 \exp\left[2\mathrm{i}k\left(l_{12} - \frac{\lambda m}{4}\right)\right] + r_3 \exp[2\mathrm{i}k(l_{12} + l_{23})]$$
$$+ r_4 \exp\left[2\mathrm{i}k\left(l_{12} + l_{23} + l_{34} + \frac{\lambda m}{4}\right)\right], \tag{33}$$

$$r = r_1 + r_2 \exp(2\mathrm{i}kl_{12}) + r_3 \exp\left[2\mathrm{i}k\left(l_{12} + l_{23} - \frac{\lambda m}{4}\right)\right]$$
$$+ r_4 \exp\left[2\mathrm{i}k\left(l_{12} + l_{23} + l_{34} - \frac{\lambda m}{4}\right)\right], \tag{34}$$

where m is an integer.

It can be seen that there are two repeating values of the total CCP. At the same time, the layout options for the PECs in question have their own characteristics. In the case of the diagonal arrangement of the PECs [relation (33)], when the perimeter is changed by λ, the vectors $\boldsymbol{r}_1$ and $\boldsymbol{r}_3$ remain fixed on the complex plane, and the vectors $\boldsymbol{r}_2$ and $\boldsymbol{r}_4$ rotate by 180°. For the second layout [relation (34)], the vectors $\boldsymbol{r}_1$ and $\boldsymbol{r}_2$ remain stationary, and the vectors $\boldsymbol{r}_3$ and $\boldsymbol{r}_4$ [the PECs mounted on mirrors (*1*) and (*2*) are rotated 180°].

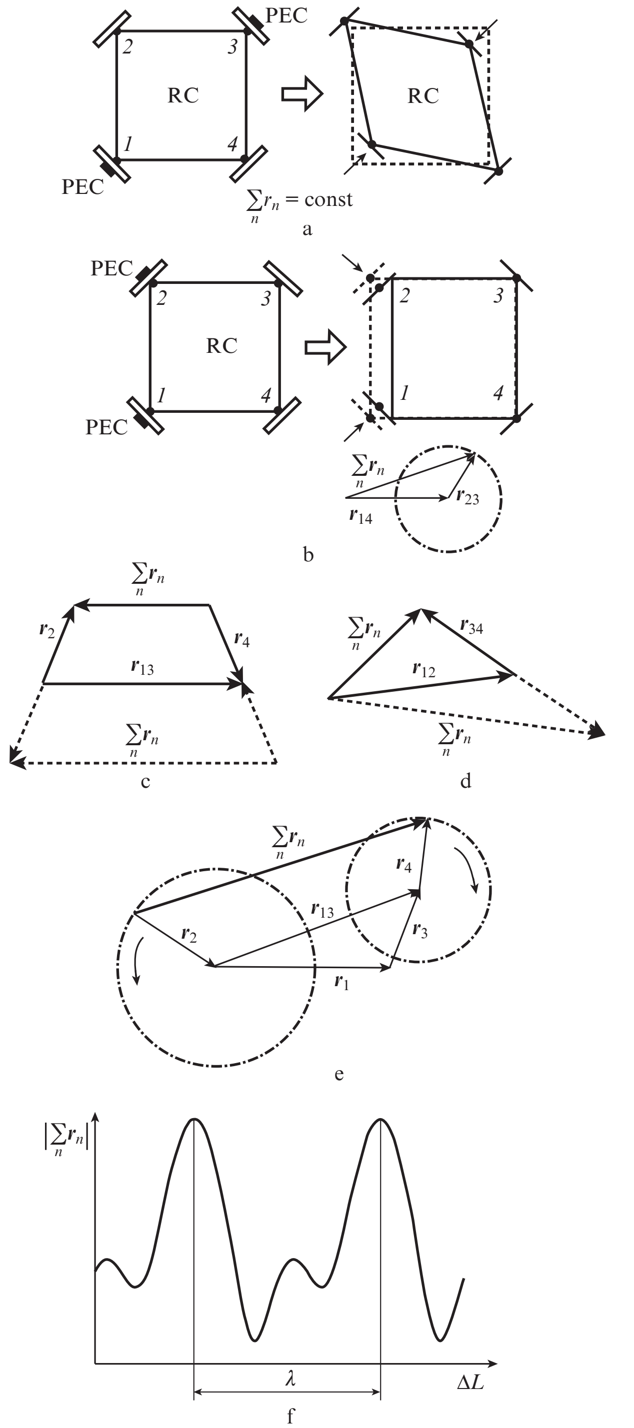

Figure 8. Formation of the total CCP in a four-mirror RC. Uniform thermal deformations: (a) diagonal arrangement of PECs and (b) PECs mounted on adjacent mirrors. Mode jump by λ: (c) diagonal arrangement, and (d) PECs mounted on adjacent mirrors. (e) Antiphase movement of two PECs with a diagonal arrangement. (f) Change in the modulus of the total CCP during the antiphase movement of two PECs.

A comparative analysis of the two layout schemes of PECs shows that a scheme with a diagonal layout is more preferable for the correction procedure implementation. Let us consider this scheme in more detail using a Zeeman LG as an example.

The main distinguishing feature of a Zeeman LG is a nonplanar RC, whose eigenmodes are circularly polarised. The frequency distance between adjacent polarisation modes is $c/(2L)$, rather than c/L, as in a planar cavity. As a result, we obtain four configurations for partial CCPs. Each of the positions of the PECs corresponds to its own pair of S_- and S_+ values. In the case of a planar RC, there are two configuration options for partial CCPs. Figure 4 shows the results of measurements of the wings of the $\Delta K(\Omega)$ dependence for one of the studied Zeeman LGs. For each of these four dependences, a pair of S_- and S_+ values is presented.

To introduce the correction procedure, it is necessary to find out how to control the configuration of partial CCPs. This makes it possible to stabilise the $\Delta K(\Omega)$ dependence for the LG. A similar approach to solving this problem was implemented by Fedorov et al. [10]. In a four-mirror RC, three mirrors were equipped with PECs. The PEC control algorithm made it possible not only to stabilise the perimeter of the cavity, but also to obtain a CCP configuration corresponding to a minimum S_+ value.

The diagonal arrangement of the PECs in a square RC allows this problem to be effectively solved. To this end, one of the PECs is used to stabilise the LG perimeter, and the movements of the other PEC stabilise the configuration of the partial CCP vectors of the mirror. This algorithm for controlling the configuration of the RC is equivalent to antiphase operation of two PECs [11]. This regime of PEC operation is shown in Fig. 8e. As the PEC moves, the vectors $\boldsymbol{r}_2$ and $\boldsymbol{r}_4$ rotate on the complex plane towards each other. The behaviour of the conservative CCP component is described by the expression

$$r = r_1 + r_2\exp(2ik\Delta l) + r_3\exp(i\vartheta_3) + r_4\exp(-2ik\Delta l + i\vartheta_4), \quad (35)$$

where Δl is the longitudinal displacement of the PEC; and ϑ_3 and ϑ_4 are the phase shifts describing the initial position of the vectors of partial conservative BS components of mirrors (*3*) and (*4*) on the complex plane. A similar relation can be written for the dissipative component.

As a result, we have periodic dependences of the CCP moduli on the parameter Δl (the period is equal to λ). Depending on the initial rotation angles on the complex plane (ϑ_3 and ϑ_4), one-humped (with one maximum) or two-humped (with two maxima) dependences of the dissipative or conservative BS components are obtained [12].

To control the configuration of the partial CCP vectors, one can use the result of measuring the modulation component of the RL intensity with the beat frequency. This parameter shows an explicit correlation with the magnitude of nonlinear corrections to the SF. Figure 9 demonstrates a nonlinear correction to the SF for a rotation velocity of 18 deg s^{-1} and the modulation intensity component during the antiphase course of two PECs as a function of the PEC voltage.

In the above example, we observed a good correlation between the nonlinear correction to the SF and the variable intensity component. This is due to the fact that in this sensor the conservative BS component significantly exceeded the dissipative component ($S_-/S_+ > 7$). If the difference is not so significant, then such a correlation is not detected. However, the magnitude of the variable component of the intensity can be used as a reference, making it possible to stabilise the configuration of the partial CCPs. Thus, the values of S_- and S_+, and hence the dependence $\Delta K(\Omega)$, can be maintained unchanged under thermal and mechanical effects of the LG.

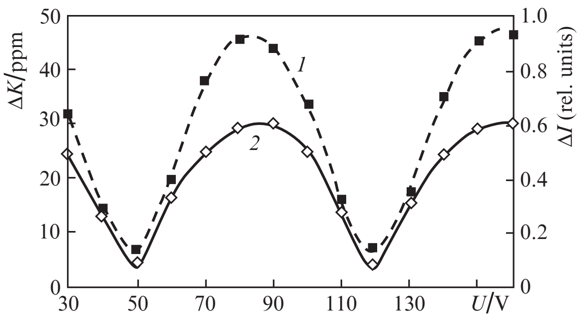

Figure 9. (*1*) Nonlinear correction to the SF ($\Omega = 18$ deg s^{-1}) and (*2*) variable component of the intensity ΔI as functions of voltage U at the PEC during the antiphase movement of two PECs. Points are the result of measurements.

4. Conclusions

Taking into account the conservative (S_-) and dissipative (S_+) CCP components of the counterpropagating waves allows one to obtain analytical relationships that well describe (quantitatively and qualitatively) nonlinear SF corrections of the LG with a rectangular bias in the entire working range of the angular velocities of the LG. In describing the wings of the $\Delta K(\Omega)$ dependence, one can neglect the influence of parametric effects and use the relations obtained in the weak-coupling approximation. In the central part of this dependence, the introduction of amplitude noise makes it possible to significantly (almost by two orders of magnitude) reduce the nonlinear distortions of the SF and to describe the shape of these corrections using the analytical relation.

Along with the S_+ and S_- parameters, the shape of the $\Delta K(\Omega)$ dependence is also determined by the amplitude of the rectangular bias and the strength of the limit cycle Ω_g of the RL. Our experiments showed that the value of Ω_g nonlinearly depends on the excess of gain over losses η. The calculated parameter Ω_g turns out to be several times larger than the measured value at $\eta > 1-2$. This casts doubt on the appropriateness of applying the system of equations (8)–(10) to describe the amplitude–phase characteristics of the RL operating at large values of η. The use of the Ω_g value obtained directly from the measurement results in the analytical $\Delta K(\Omega)$ dependence allows one to correctly describe the magnitude of the nonlinear corrections to the SF caused by the BS effects.

The diagonal arrangement of PECs in the RC of square cross section makes it possible to effectively control the configuration of partial CCP mirrors. As a reference, one can use the amplitude of the variable component of the CPW intensity with the beat frequency, reaching its minimum value when moving PECs. According to our estimates, such an approach to the corrections of nonlinear corrections in LGs with a rectangular bias, caused by the BS effects, will reduce them to 1–2 ppm.

References

1. Aronowitz F., Collins R.J. *Appl. Phys. Lett*., **9**, 55 (1966).
2. Aronowitz F., in *Optical Gyros and their Application*s (Neuilly-sur-Seine, France, RTO AGARDograph 339, 1999) p. 3.1.
3. Klimontovich Yu.L. (Ed.) *Volnovye i fluktatsionnye protsessy v lazerakh* (Wave and Fluctuation Processes in Lasers) (Moscow: Nauka, 1974).
4. Azarova V.V., Golyaev Yu.D., Dmitriev V.G. *Quantum Electron*., **30**, 96 (2010) [*Kvantovaya Elektron*., **30**, 96 (2010)].
5. Azarova V.V., Golyaev Yu.D., Saveliev I.I. *Quantum Electron*., **45**, 171 (2015) [*Kvantovaya Elektron.*, **45**, 171 (2015)].
6. Khoshev I.M. Cand. Thesis (Moscow: Lomonosov Moscow State University, 1978).
7. Gorshkov V.N., Grushin M.E., Lariontsev E.G., Saveliev I.I., Khokhlov N.I. *Quantum Electron*., **46**, 1061 (2016) [*Kvantovaya Elektron*., **46**, 1061 (2016)].
8. Etrich C., Mandel P., CentenoNeelen R., Spreeuw R.J.C., Woerdman J.P. *Phys. Rev. A*, **46**, 525 (1992).
9. Birman A.Ya., Petrukhin EA, Savushkin A.F. *Sov. J. Quantum Electron*., **9**, 1557 (1979) [*Kvantovaya Elektron*., **6**, 2626 (1979)].
10. Fedorov A.E., Zborovskii V.A., Rekunov D.A., Kurylev A.N. *Proc. XXIV St. Petersburg Int. Conf. on Integrated Navigation Systems* (St. Petersburg, 2017) pp 349–355.
11. Bessonov A.S., Makeev A.P., Petrukhin E.A. *Quantum Electron*., **47**, 675 (2017) [*Kvantovaya Elektron*., **47**, 675 (2017)].
12. Bessonov A.S., Makeev A.P., Petrukhin E.A. *Proc. XXIV St. Petersburg Int. Conf. on Integrated Navigation Systems* (St. Petersburg, 2017) pp 482–486.